
Transformer-like Inference from Optimal Control

Aditya Kudre
 Coordinated Science Laboratory
 Electrical and Computer Engineering
 University of Illinois Urbana-Champaign

Heng-Sheng Chang*
 Coordinated Science Laboratory
 Mechanical Science and Engineering
 University of Illinois Urbana-Champaign

Prashant G. Mehta
 Coordinated Science Laboratory
 Mechanical Science and Engineering
 University of Illinois Urbana-Champaign

Abstract

Decoder-only transformers compute the conditional probability of the next token from a sequence of past observations. This paper derives, from first principles, inference architectures that solve the same prediction problem — and in doing so, recovers transformer-like layer operations as a consequence of optimal control theory. The framework is developed for two model classes: a nonlinear model of discrete-valued processes, directly motivated by the transformer, and a linear Gaussian model as a tractable baseline. For both model classes, the prediction objective is reformulated as an optimal control problem whose solution yields an explicit inference algorithm, the dual filter, with a layer structure that mirrors the layer structure of a decoder-only transformer. Numerical experiments provide a comparison of the optimal control to attention weights from a trained transformer. These experiments reveal that when the embedding dimension is insufficient, the transformer implicitly exploits non-Markovian structure.

1 Introduction

A decoder-only transformer computes the conditional probability of the next token through a sequence of L identical layer operations:

$$\text{(Layer for transformer)} \quad [\sigma_1, \sigma_2, \dots, \sigma_T]_{d \times T} \mapsto [\sigma_1^+, \sigma_2^+, \dots, \sigma_T^+]_{d \times T}, \quad (1a)$$

where each layer maps a $(d \times T)$ -sequence of (embedding) vectors to a $(d \times T)$ -sequence of the same dimension, with σ_t^+ depending only on $\{\sigma_1, \dots, \sigma_t\}$ (causal structure), for $1 \leq t \leq T$ [1]. The output of the final layer is decoded to give the next-token prediction. This layer structure is the defining architectural feature of the transformer — yet its mathematical justification remains unclear. Why should the optimal prediction architecture take this particular form?

This paper offers one answer using optimal control theory. We adopt a model-based approach where the observed tokens are generated from an underlying hidden stochastic process, and the prediction problem is cast as causal inference in a partially observed system:

$$\begin{aligned} \text{(hidden state process)} \quad X &:= [X_0, X_1, \dots, X_T] \quad \text{taking values in state-space } \mathbb{S}, \\ \text{(observation process)} \quad Z &:= [Z_1, Z_2, \dots, Z_T, Z_{T+1}] \quad \text{taking values in observation-space } \mathbb{O}, \end{aligned}$$

where the joint distribution of (X, Z) is according to the probabilistic graphical model in Fig. 1. We consider two model classes, based on definition of \mathbb{S} and \mathbb{O} , as described in Table 1.

*Corresponding author email: hschang@illinois.edu

Table 1: Two model classes: For the nonlinear model, the prediction is the conditional probability of the hidden state. For the linear Gaussian model, the prediction is the conditional expectation of the hidden state.

Models	State-space \mathbb{S}	Observation-space \mathbb{O}	Prediction	Motivation
Nonlinear	$\{1, 2, \dots, d\}$	$\{0, 1, \dots, m\}$	$\pi_T := \mathbb{P}(X_T Z_{1:T})$	transformer-like
Linear	\mathbb{R}^d	\mathbb{R}^m	$\hat{X}_T := \mathbb{E}(X_T Z_{1:T})$	tractable baseline

Table 2: Inference architectures for the two model classes: The prediction is computed as a weighted sum of past observations. In the nonlinear predictor, weights are causally adapted to the observation data (i.e., U_t is allowed to depend upon $Z_{1:t}$). This data-dependence is what makes the predictor nonlinear and is the direct analogue of attention weights in a transformer.

	Representation	Weights (or control)
Nonlinear predictor (for nonlinear model)	$\pi_T(f) = (\text{const.}) - \sum_{t=1}^T U_{t-1}^\top e(Z_t),$ for $f : \mathbb{S} \rightarrow \mathbb{R}.$	$U = \{U_0, \dots, U_{T-1}\}$ is an \mathbb{R}^m -valued adapted process
Linear predictor (for linear model)	$f^\top \hat{X}_T = (\text{const.}) - \sum_{t=1}^T u_{t-1}^\top Z_t,$ for $f \in \mathbb{R}^d.$	$u = \{u_0, u_1, \dots, u_{T-1}\}$ is an \mathbb{R}^m -valued deterministic process

The nonlinear model setting is directly motivated by the transformer: \mathbb{O} is the vocabulary, and $|\mathbb{S}| = d$ is the embedding dimension. The prediction of interest is the conditional probability $\pi_T(\cdot) := \mathbb{P}(X_T = \cdot | Z_{1:T})$, a probability vector of dimension d , from which the next-token prediction $\mathbb{P}(Z_{T+1} = \cdot | Z_{1:T})$ is computed. The linear Gaussian model serves as a tractable baseline in which exact, closed-form results are available. The same notation (X, Z) is used for both model classes; the appropriate class will be clear from context.

Our objective is to derive transformer-inspired inference architectures where the prediction — conditional probability for the nonlinear model and conditional expectation for the linear model — is computed as a causal transformation of $Z_{1:T}$. The representations are formally introduced in Table 2.

A key finding is that for both model classes, the optimal predictor is computed by iterating a $d \times T$ sequence-to-sequence transformation — structurally analogous to a transformer layer, but derived here from optimality conditions of the prediction problem rather than specified by architecture.

While the representation for the linear predictor is standard for the Gaussian processes, the representation for the nonlinear predictor is an original contribution of this paper (Prop. 4 gives well-posedness — existence and uniqueness — of U). The other original contributions are as follows:

Optimal control framework for computing weights. For both model classes, the synthesis of optimal weights — u for the linear predictor and U for the nonlinear predictor — is formulated as an optimal control problem (OCP).

For the linear model, the OCP is solved for the general non-Markovian X , yielding a non-recursive algorithm that is provably more efficient than the recursive Kalman filter architecture ($O(T^2 d^2)$ vs $O(T^3 d^2)$). For the nonlinear model, the OCP and explicit formula for U are obtained only for the Markovian X , i.e., when (X, Z) is a hidden Markov model (HMM), with complexity $O(T^2 d^2)$ — same as a transformer layer — independent of vocabulary size m .

Transformer-like layer operation. The OCP solution defines a layer transformation on a $d \times T$ -sequence — directly analogous to the transformer. For the linear model, the $(d \times T)$ -sequence is the momentum process, and the layer transformation is defined using Pontryagin’s maximum principle:

$$\text{(Layer for linear predictor)} \quad [\eta_0, \dots, \eta_{T-1}]_{d \times T} \xrightarrow{\text{(Hamilton's equation)}} [\eta_0^+, \dots, \eta_{T-1}^+]_{d \times T}. \quad (1b)$$

At convergence, the layer transformation yields the optimal momentum sequence, from which the prediction weights u are computed via an explicit formula.

For the nonlinear model (analysis is limited to HMM), the layer maps the probability sequence:

$$\text{(Layer for nonlinear predictor)} \quad [\rho_1, \dots, \rho_T]_{d \times T} \xrightarrow{\text{(optimality equation)}} [\rho_1^+, \dots, \rho_T^+]_{d \times T}. \quad (1c)$$

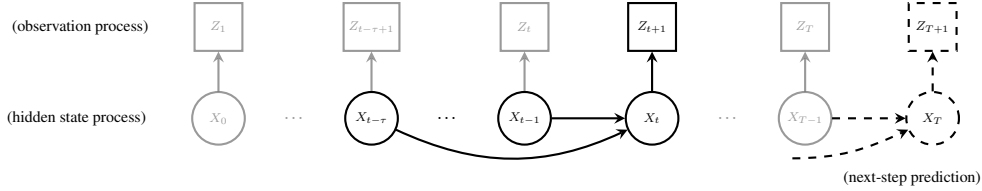


Figure 1: Graphical model for (X, Z) . For $\tau = 1$, X is a Markov process and (X, Z) is a hidden Markov model (HMM). For $\tau > 1$, X is a non-Markovian (or a τ^{th} -order Markov) process. For $\tau = T$, X_T depends upon the entire past $X_{0:T-1}$.

At convergence, the layer transformation yields the conditional probability of the hidden state at each time step, from which the weights U are computed via an explicit formula. For both models, the layer transformation emerges from the optimality conditions rather than being specified by architecture.

Numerical experiments provide a direct side-by-side comparison of optimal control weights and attention weights from a trained nanoGPT (Fig. 3). When the embedding dimension is insufficient, the dual filter degrades while nanoGPT retains near-optimal performance — revealing that the transformer implicitly exploits non-Markovian structure.

Related work. Prior work on mathematical modeling of transformers interpret the architecture as a transport on probability measures [2, 3, 4, 5, 6]. Building on these perspectives, optimal control formalisms have been applied to analysis and learning [7, 8, 9, 10]. A complementary perspective is based on Bayesian inference including HMM and nonlinear filtering [11, 12, 13, 14, 15, 16, 17, 18]. The present paper builds directly on [18] but differs from other works, which focus on interpreting and refining attention mechanisms rather than modeling the prediction problem from first principles based on the representations introduced in Table 2.

The remainder of this paper is organized as follows: The OCPs for the linear and the nonlinear models are described in Sec. 2 and Sec. 3, respectively. The numerical experiments are presented in Sec. 4 and the paper closes with conclusions in Sec. 5.

2 Linear Gaussian Model

Consider the graphical model in Fig. 1 for the case when (X, Z) is an $\mathbb{R}^d \times \mathbb{R}^m$ -valued Gaussian process, with state-space representation:

$$X_{t+1} = \sum_{s=1}^{\min(\tau, t+1)} A_{t+1,s} X_{t+1-s} + B_{t+1}, \quad 0 \leq t \leq T-1, \quad X_0 \sim \mathcal{N}(\mu_0, \Sigma_0), \quad (2a)$$

$$Z_{t+1} = C X_t + W_{t+1}, \quad 0 \leq t \leq T, \quad (2b)$$

where τ is the model-order parameter, $C \in \mathbb{R}^{m \times d}$ is the observation matrix, and $A_{\cdot, \cdot} \in \mathbb{R}^{d \times d}$ are the state transition matrices. Stochasticity is introduced through three mutually independent sources: (1) the Gaussian initial condition $X_0 \sim \mathcal{N}(\mu_0, \Sigma_0)$, (2) the white Gaussian noise (WGN) process $B_t \sim \mathcal{N}(0, Q)$ with $Q \succeq 0$, and (3) the WGN process $W_t \sim \mathcal{N}(0, R)$ with $R \succ 0$, for $1 \leq t \leq T$.

The goal is to compute the conditional expectation $\hat{X}_T := \mathbb{E}(X_T | Z_{1:T})$, from which the next-step prediction $\mathbb{E}(Z_{T+1} | Z_{1:T}) = C \hat{X}_T$ is readily computed.

For the fully non-Markovian case (with $\tau = T$), a Kalman filter needs to maintain an estimate, conditional mean and covariance, of the entire history $\{X_0, X_1, \dots, X_t\}$ at each time t [19, Ch. 8.2]. The size of this data structure grows with t — $O(td)$ for the conditional mean and $O(t^2 d^2)$ for the conditional covariance — leading to $O(T^3 d^2)$ total complexity over the time-horizon (Table 3). This motivates the question: is a more efficient algorithm possible with a fixed $d \times T$ data structure, as in a transformer? The answer is affirmative — the OCP formulation below yields such an algorithm.

2.1 Optimal control problem (OCP) for computing weights

The OCP is formulated as follows. Consider the space of admissible control inputs as

$$\text{(admissible control)} \quad \mathcal{U}^{(\text{det})} := \{u_t : u_t \in \mathbb{R}^m, 0 \leq t \leq T-1\}.$$

For any given $f \in \mathbb{R}^d$ and a deterministic control sequence $u \in \mathcal{U}^{(\text{det})}$, define the \mathbb{R}^d -valued backward process $y = \{y_t : y_t \in \mathbb{R}^d, 0 \leq t \leq T\}$ by

$$\text{(dual control system)} \quad y_t = \sum_{s=1}^{\min(\tau, T-t)} A_{t+s,s}^\top y_{t+s} + C^\top u_t, \quad 0 \leq t \leq T-1, \quad y_T = f, \quad (3)$$

and the associated optimal-control cost functional

$$\text{(optimal control objective)} \quad J_T(u; f) := \frac{1}{2} |y_0|_{\Sigma_0}^2 + \frac{1}{2} \sum_{t=0}^{T-1} (|y_{t+1}|_Q^2 + |u_t|_R^2).$$

Proposition 1 (Duality principle for non-Markovian linear Gaussian model). *Consider an estimator*

$$S_T := \mu_0^\top y_0 - \sum_{t=1}^T u_{t-1}^\top Z_t,$$

where y_0 is obtained from (3) with $u \in \mathcal{U}^{(\text{det})}$ and $y_T = f$. Then

$$J_T(u; f) = \mathbb{E} \left(\frac{1}{2} |f^\top X_T - S_T|^2 \right). \quad (4)$$

Proof. See Sec. B.1 in the appendix. ■

The right-hand side of (4) is the mean-squared error (MSE). The duality principle relates the MSE to an optimal control objective: the control u that minimizes $J_T(u; f)$ yields the MMSE estimator, which for Gaussian processes equals the conditional mean $f^\top \hat{X}_T$. This motivates the following optimal control problem:

$$\text{(OCP)} \quad \min_{u \in \mathcal{U}^{(\text{det})}} J_T(u; f) \quad \text{subject to (3)} \quad (5)$$

Theorem 2 (Optimal control formula). *Consider the OCP (5). Then there exists a unique optimal control sequence $u^{(\text{opt})} \in \mathcal{U}^{(\text{det})}$, given by the following forward-backward system:*

$$\text{(backward)} \quad y_t = \sum_{s=1}^{\min(\tau, T-t)} A_{t+s,s}^\top y_{t+s} + C^\top u_t^{(\text{opt})}, \quad y_T = f, \quad (6a)$$

$$\text{(forward)} \quad \eta_t = \sum_{s=1}^{\min(\tau, t)} A_{t,s} \eta_{t-s} + Q y_t, \quad \eta_0 = \Sigma_0 y_0, \quad (6b)$$

$$\text{(optimal control formula)} \quad u_t^{(\text{opt})} = -R^{-1} C \eta_t, \quad t = 0, 1, \dots, T-1. \quad (6c)$$

Proof. See Sec. B.2 in the appendix. ■

Thm. 2 justifies equation (1b) for the layer operation introduced in Sec. 1. The momentum process $\eta := \{\eta_t : 0 \leq t \leq T-1\}$ is a $d \times T$ data structure, and a single backward-forward pass of (6) defines the layer transformation $\eta \mapsto \eta^+$ in (1b). Complexity comparison with the Kalman filter appears in Table 3. We refer to the algorithm as the dual filter.

Related work. State space models such as Mamba invoke a duality between recurrent and convolutional representations to derive efficient sequential architectures [20]. The duality in this paper is of a different character: it is between optimal filtering and optimal control [21, 22], yielding inference architectures from first principles rather than from architectural design. For the Markovian case ($\tau = 1$), the duality is classical and referred to as Kalman's or minimum-variance duality [23, p. 180] [24, p. 100], [25]. See [26] for a historical overview of duality in control theory.

This linear analysis sets the stage for the nonlinear model presented next.

Table 3: Complexity of the inference algorithm for the non-Markovian (model order $\tau = T$) linear Gaussian model (2).

Algorithm	Time	Memory	Data structure
Recursive Kalman filter	$O(T^3 d^2)$	$O(T^2 d^2)$	Growing mean and covariance matrices
Dual filter (non-recursive)	$O(T^2 d^2)$	$O(Td)$	Fixed $d \times T$
Transformer (per layer)	$O(T^2 d^2)$	$O(Td)$	Fixed $d \times T$

3 Nonlinear Model

Consider the graphical model in Fig. 1 with discrete state-space $\mathbb{S} = \{1, 2, \dots, d\}$ and observation-space $\mathbb{O} = \{0, 1, 2, \dots, m\}$ (see Table 1). The next observation Z_{t+1} depends on the past only through the current state X_t , with conditional distribution

$$P(Z_{t+1} = z | X_t = x) = C(x, z), \quad x \in \mathbb{S}, \quad z \in \mathbb{O}, \quad 0 \leq t \leq T - 1, \quad (7a)$$

where $C \in \mathbb{R}^{d \times (m+1)}$ is a row stochastic matrix. The column vector $C(\cdot, z)$ is the probabilistic analogue of the embedding vector for token z in a transformer.

The prediction target is the conditional probability $\pi_T(x) := P(X_T = x | Z_{1:T})$ for $x \in \mathbb{S}$. The next-token prediction is then readily computed as

$$P(Z_{T+1} = z | Z_{1:T}) = \pi_T(C(\cdot, z)) := \sum_{x \in \mathbb{S}} \pi_T(x) C(x, z), \quad z \in \mathbb{O}.$$

This computation is the probabilistic analogue of the un-embedding operation in a transformer.

The main result of this section is the nonlinear predictor representation for π_T , formally introduced in Table 2, whose well-posedness is established in Prop. 4 below. The representation involves a mapping $e : \mathbb{O} \rightarrow \mathbb{R}^m$ defined as follows:

$$e(1) = \begin{bmatrix} 1 \\ 0 \\ \vdots \\ 0 \end{bmatrix}_{m \times 1}, \quad e(2) = \begin{bmatrix} 0 \\ 1 \\ \vdots \\ 0 \end{bmatrix}_{m \times 1}, \quad \dots, \quad e(m) = \begin{bmatrix} 0 \\ 0 \\ \vdots \\ 1 \end{bmatrix}_{m \times 1}, \quad e(0) = -e(1) - e(2) - \dots - e(m).$$

Here $e(z)$ for $z = 1, 2, \dots, m$ is the one-hot encoding, and $e(0)$ is chosen so that $\sum_{z \in \mathbb{O}} e(z) = 0$.

Example 3 ($m=1$). Suppose the observations are binary-valued, i.e., $\mathbb{O} = \{0, 1\}$. Then

$$e(1) = 1, \quad e(0) = -1.$$

In the nonlinear setting, the space of admissible weight sequences is

$$\mathcal{U} := \{U_t \in \mathbb{R}^m : U_t \text{ is measurable w.r.t. } \mathcal{Z}_t, \quad 0 \leq t \leq T - 1\},$$

where $\mathcal{Z}_t := \sigma(\{Z_s : 1 \leq s \leq t\})$ is the sigma-algebra generated by observations up to time t with \mathcal{Z}_0 the trivial sigma-algebra. In words, U_t is required to depend only on past observations Z_1, Z_2, \dots, Z_t — a causal dependence condition analogous to the causal masking in a decoder-only transformer. Note the contrast with $\mathcal{U}^{(\text{det})}$: the weights are now random (data-dependent) rather than deterministic, which is what makes the predictor nonlinear.

Proposition 4 (Nonlinear predictor representation). Fix $f : \mathbb{S} \rightarrow \mathbb{R}$. There exists $U \in \mathcal{U}$ such that

$$\pi_T(f) = (\text{const.}) - \sum_{t=1}^T U_{t-1}^\top e(Z_t), \quad \text{P-a.s.}$$

If $P(Z_1 = z_1, \dots, Z_T = z_T) > 0$ for all $(z_1, \dots, z_T) \in \mathbb{O}^T$, then U is unique.

Proof. See Sec. B.3 in the appendix. ■

The nonlinear predictor representation in Prop. 4 reduces the prediction problem to the synthesis of the weight sequence $U \in \mathcal{U}$. As in the linear Gaussian model, this synthesis is formulated as an optimal control problem. In the following, the results are described for the Markovian case ($\tau = 1$), i.e., when (X, Z) is an HMM. Unlike the linear Gaussian model where the OCP is solved for the general non-Markovian model, an explicit formula for U is obtained here only for $\tau = 1$.

Table 4: Key objects in the nonlinear OCP and their linear Gaussian analogues.

Object	Definition	Role	Linear analogue
$U \in \mathcal{U}$	\mathbb{R}^m -valued adapted process	Control/weights	$u \in \mathcal{U}^{(\text{det})}$
$f : \mathbb{S} \rightarrow \mathbb{R}$	Function on \mathbb{S}	Prediction target is $\pi_T(f)$	$f \in \mathbb{R}^d$
(Y, V)	Solution of BS Δ E (with $U, Y_T = f$)	Dual process	y (backward process)
$J_T(U; f)$	Optimal control objective	MSE of estimator S_T	$J_T(u; f)$

3.1 Optimal control problem (OCP) for computing weights

The remainder of this section is closely adapted from [18]. We make the following assumption:

Assumption 5 (Hidden Markov Model). *The pair (X, Z) is a hidden Markov model (HMM) with emission matrix C as defined in (7a), and state transition:*

$$\mathbb{P}(X_0 = x) = \mu(x), \quad \mathbb{P}(X_{t+1} = x' \mid X_t = x) = A(x, x'), \quad x, x' \in \mathbb{S}, \quad t = 0, 1, \dots, T-1, \quad (7b)$$

where $A \in \mathbb{R}^{d \times d}$ is a row stochastic matrix.

The optimal control formulation for the HMM parallels that of the linear Gaussian model in Sec. 2, with the key objects summarized in Table 4. For the HMM, the dual control system is a backward stochastic difference equation (BS Δ E) whose solution is denoted by (Y, V) where Y is a stochastic process whose linear analogue is the deterministic dual process y . The auxiliary process V has no analogue in the linear case; the process enforces adaptedness of Y to the filtration \mathcal{Z}_t . The explicit formulae for these and the optimal control objective $J_T(U; f)$ appear in Sec. A of the appendix.

Proposition 6 (Duality principle for HMM [18, Theorem 9]). *Consider an estimator*

$$S_T := \mu(Y_0) - \sum_{t=0}^{T-1} U_t^\top e(Z_{t+1}),$$

where Y_0 is obtained from the BS Δ E (10) with $U \in \mathcal{U}$ and $Y_T = f$. Then

$$J_T(U; f) = \mathbb{E} \left(|f(X_T) - S_T|^2 \right).$$

Consequently, minimizing $J_T(U; f)$ over $U \in \mathcal{U}$ yields the MMSE estimator $\pi_T(f)$.

The duality principle reduces weight synthesis to the following optimal control problem:

$$\text{(OCP)} \quad \min_{U \in \mathcal{U}} J_T(U; f) \quad \text{subject to BS}\Delta\text{E (10) in Sec. A.} \quad (8)$$

Denote the conditional probability of the hidden state X_t at time t as $\pi_t(x) := \mathbb{P}(X_t = x \mid Z_{1:t})$, $x \in \mathbb{S}$, for $1 \leq t \leq T$. The solution of (8) yields a fixed-point representation of the conditional probability process $\pi = \{\pi_t : 1 \leq t \leq T\}$, as described in the following theorem.

Theorem 7 (Formula for optimal control [18, Theorem 11]). *Consider (8). Then an optimal control $U^{(\text{opt})} = \{U_t^{(\text{opt})} : 0 \leq t \leq T-1\}$ is of the feedback form given by*

$$\text{(optimal control law)} \quad U_t^{(\text{opt})} = \phi(Y_t, V_t; \pi_t), \quad \text{P-a.s.}, \quad 0 \leq t \leq T-1. \quad (9a)$$

(See equation (A) in Sec. A for an explicit form for $\phi : \mathbb{R}^d \times \mathbb{R}^{m \times d} \times \mathbb{R}^d \rightarrow \mathbb{R}^m$). Suppose $(Y^{(\text{opt})}, V^{(\text{opt})})$ is the solution of the BS Δ E with $U = U^{(\text{opt})}$. Then

$$\pi_s(Y_s^{(\text{opt})}) = \mu(Y_0^{(\text{opt})}) - \sum_{t=1}^s (U_{t-1}^{(\text{opt})})^\top e(Z_t), \quad \text{P-a.s.}, \quad 1 \leq s \leq T. \quad (9b)$$

Thm. 7 justifies the layer transformation (1c) introduced in Sec. 1. Eq. (9b) shows that the optimal control $U^{(\text{opt})}$ yields a causal representation of the conditional probability process π : At a query time-step s , the prediction π_s is computed in terms of the weights $\{U_{t-1}^{(\text{opt})} : 1 \leq t \leq s\}$ (see Fig. 3). Moreover, since $U_t^{(\text{opt})} = \phi(Y_t, V_t; \pi_t)$ depends on π_t through (9a), equation (9b) is a fixed-point representation of π . This fixed-point structure defines a natural layer transformation: given an approximation $\rho \approx \pi$ as input, one pass through the BS Δ E, using the control law (9a) with ρ_t instead of π_t , produces an updated approximation ρ^+ as output.

Related work. Relative to [18], the novel contributions of this paper are: (i) the nonlinear predictor representation (Prop. 4), which is proved here for the general non-Markovian model; and (ii) the parallel treatment of the nonlinear and linear Gaussian models within a unified optimal control framework. The explicit formula for U is given only for the Markovian case ($\tau = 1$), based on the original derivation of the same in [18]. The numerical experiments in Sec. 4 suggest that extending the framework to the non-Markovian case ($\tau > 1$) is both important and feasible — a transformer implicitly solves this problem through attention, and the dual filter framework provides a mathematical foundation for a principled extension.

4 Numerical Experiments

The observation process $Z = \{Z_t : 1 \leq t \leq T\}$ takes values in $\mathbb{O} = \{0, 1\}$ (i.e. binary observations $m = 1$) and is constructed by concatenating two types of deterministic patterns:

$$z^{\text{long}} = \{1, 1, \underbrace{0, \dots, 0}_{(d-2) \text{ zeros}}\}, \quad z^{\text{short}} = \{1, \underbrace{0, \dots, 0}_{q \text{ zeros}}\},$$

where d is the length of the long pattern and $q < d - 2$ is the number of zeros in the short pattern. At the end of each cycle, the next pattern type (long or short) is selected independently with probability 0.5, and the corresponding pattern is appended.

The stochastic process Z is a d -th order Markov process: The conditional probability of Z_t depends on the position within the current cycle, which in the worst case (a long cycle) requires knowledge of up to the past d observations. A minimal HMM representation on state-space $\mathbb{S} = \{1, 2, \dots, d\}$ is depicted in Fig. 2 together with a sample path of Z showing the two types of patterns.

Remark 8. *The choice of two patterns is deliberate: all predictive information is carried by the 1s, which are sparse and always surrounded by a long string of zeros. This raises two questions: whether a fully trained nanoGPT focuses its attention weights on the 1s, and how those attention weights compare structurally to the optimal control weights.*

We have three goals in this study:

1. Evaluate the attention weights using a decoder-only transformer (nanoGPT) with its embedding dimension set to d .
2. Evaluate the optimal control weights using the dual filter with the true HMM parameters, and compare their structure to the attention weights.
3. Evaluate the effect of the candidate state dimension \hat{d} on inference performance. The HMM parameters are learned via Baum-Welch for each \hat{d} , covering the undercomplete ($\hat{d} < d$), matched ($\hat{d} = d$), and overcomplete ($\hat{d} > d$) regimes.

In the numerical experiments reported below, we fix $d = 16$, $q = 4$, and $T = 64$. (Results are qualitatively similar for other values of d and T , as described in Sec. C.3.) The performance is assessed using the cross-entropy loss of next-token prediction. Because the data is generated from a known HMM, the optimal (minimum) loss equals the conditional entropy under the true nonlinear filter, which serves as the benchmark throughout.

4.1 Comparison of attention and control weights

A nanoGPT [27] with one layer, one attention head, and embedding dimension d achieves near-optimal loss (see Appendix C for training details).

In the model-based setting, the optimal control weights are computed using the formula derived in Sec. 3. Fig. 3 depicts a side-by-side comparison of the attention weights and the control weights. Qualitatively, both sets of weights show a sparse pattern which is non-zero at the time indices when 1s are seen in the data. There is a simple explanation for sparsity and structure of the control weights. The control is non-zero only following those time-indices t such that $X_t = d$ with associated emission $Z_{t+1} = 1$. At the branching point, the filter splits equally between the two possible next states: the filter $\pi_{t+1}(x) = \frac{1}{2}(\delta_1(x) + \delta_{d-q}(x))$, yielding a non-zero value $U_{t+1}^{(\text{op})}$. At all other time-indices, the filter has its probability mass only on one state with associated control as 0.

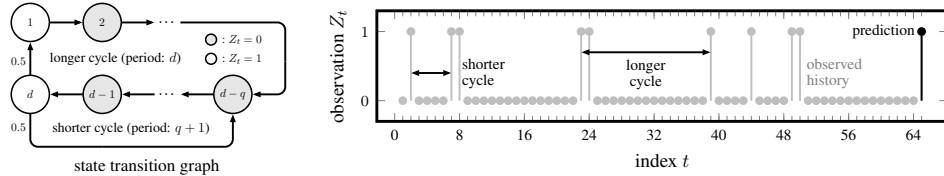


Figure 2: Two-cycle HMM and a sample observation sequence. (left) State transition graph: state d branches with equal probability into a long cycle or a short cycle, merging at state $d - q$ before returning to state d . States 1 and d emit $Z_t = 1$; all others emit $Z_t = 0$. (right) Sample trajectory with observed history indicated as gray and the prediction target as black.

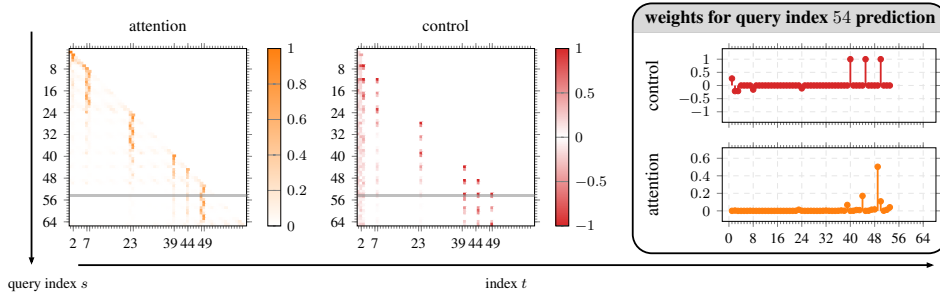


Figure 3: Attention and control weight heatmaps for $d = \hat{d} = 16$ and $T = 64$. (left) Attention matrix from a trained nanoGPT: sparse, concentrated at time indices where $Z_t = 1$. (middle) Dual filter control weights computed with exact HMM parameters: same sparsity pattern, non-zero only where $Z_t = 1$. (right) Slice at the query step $s = 54$: control (top) and attention (bottom) both focus on time indices where $Z_t = 1$, for $1 \leq t \leq s$. The corresponding query step is highlighted in the attention and control heatmaps with a horizontal gray background. The major ticks in the index axis of the heatmaps correspond to the time indices where $Z_t = 1$; the minor ticks correspond to the time indices where $Z_t = 0$.

These results demonstrate that the transformer has learned, without any knowledge of the HMM, a weighting structure that qualitatively resembles the optimal control weights derived from first principles. The more interesting regime is when the embedding dimension is smaller than the true (Markovian) state dimension. This is the subject of the following experiment.

4.2 Effect of dimension \hat{d} (non-Markovian advantage)

In this experiment, the performance of the dual filter and nanoGPT are evaluated as the candidate state dimension \hat{d} is varied. The true state dimension is fixed at $d = 16$, and \hat{d} is tested both below and above d . For each \hat{d} , including for $\hat{d} = d$, the HMM parameters (A, C) are estimated from data using the Baum-Welch algorithm; the same dataset is used to train nanoGPT.

For $\hat{d} \geq d$, both methods achieve near-optimal performance. The more interesting regime is $\hat{d} < d$, where the dual filter’s Markovian model fails to capture the full temporal structure of the observations, resulting in performance degradation. In contrast, nanoGPT maintains near-optimal performance even at $\hat{d} = d/2$, implicitly leveraging non-Markovian structure through its attention mechanism.

Fig. 4 shows the attention weights at three representative values: $\hat{d} \in \{8, 16, 32\}$. Across all three values, the attention weights consistently focus on time indices where $Z_t = 1$, identifying the informative observations regardless of model misspecification. This gap — the dual filter degrades while nanoGPT does not — is precisely the *non-Markovian advantage* [28]: the transformer implicitly operates beyond the Markovian regime, motivating the extension of the dual filter to the non-Markovian nonlinear case as a direction for future work.

4.3 Sparsity of attention and control weights

Transformer architectures are designed to produce sparse attention weights, but whether sparsity is optimal remains unclear. In the two-cycle HMM, deterministic emissions cause the filter to collapse to a point mass except at the branching state, yielding sparse optimal control weights with a vertical pattern — nonzero only immediately after $X_t = d$.

A perturbation study reveals a qualitative shift in the optimal control structure (Sec. C.2 in Appendix). Even small perturbations to the transition parameter A induce a sparse but diagonal pattern, aggregating evidence across multiple past cycles rather than relying on a single branching moment (Fig. 6 in Sec. C.2). In contrast, the nanoGPT attention weights remain sparse and vertical across perturbations, while still closely matching the optimal loss of the dual filter.

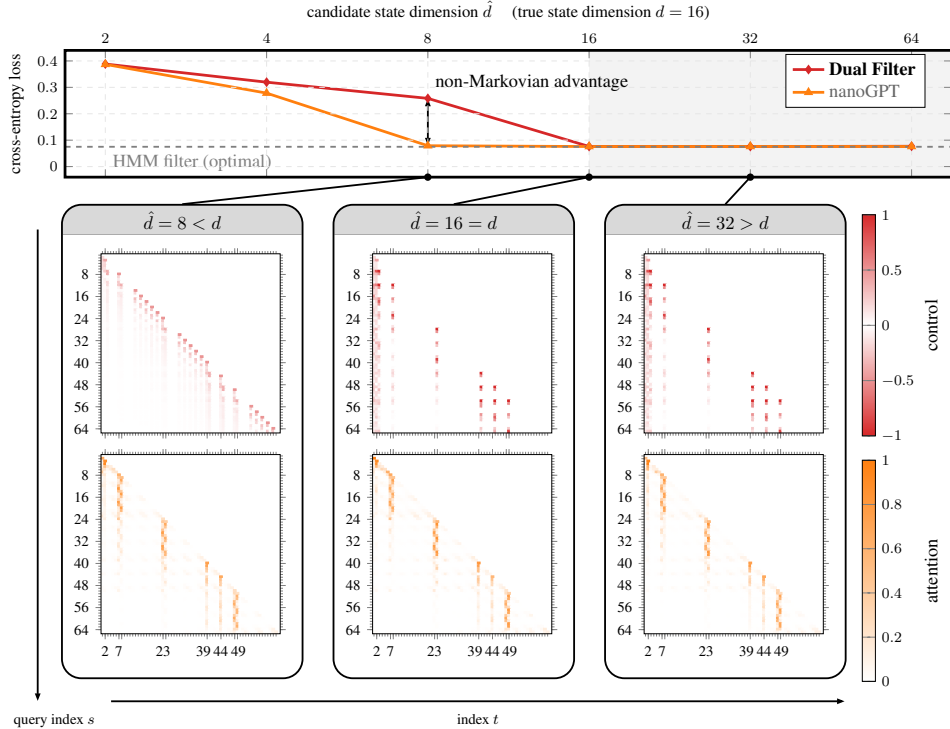


Figure 4: Non-Markovian advantage. (top) Cross-entropy loss vs. \hat{d} for the dual filter and nanoGPT; dashed line is the HMM filter. (bottom) Control and attention heatmaps at $\hat{d} \in \{8, 16, 32\}$; color intensity indicates weight magnitude. The major ticks in the index axis correspond to the time indices where $Z_t = 1$; the minor ticks correspond to the time indices where $Z_t = 0$. When $\hat{d} < d$, controls degrade while attentions remain focused on $Z_t = 1$, revealing the non-Markovian advantage.

We caution against over-interpreting weight structure: performance and weight pattern are distinct. In the non-Markovian advantage of Fig. 4, the dual filter’s degradation in the undercomplete regime is a capacity issue, not a consequence of the attention weight structure. On the other hand, Fig. 6 shows that the transformer achieves near-optimal loss even in the perturbed case. Whether sparse attention is what enables nanoGPT to robustly exploit non-Markovian structure remains an open question.

5 Conclusion

This paper derives transformer-like inference architectures from first principles using optimal control theory. For two model classes — a linear Gaussian model and a nonlinear discrete-valued model — the prediction objective is reformulated as an optimal control problem whose solution defines a $d \times T$ sequence-to-sequence transformation, structurally analogous to a transformer layer, emerging from optimality conditions rather than specified by architecture.

Numerical experiments provide a direct comparison of optimal control weights and attention weights from a trained nanoGPT. In the matched regime ($\hat{d} = d$), the two weight structures are qualitatively aligned — both sparse and focused on the informative observations. In the undercomplete regime ($\hat{d} < d$), the dual filter degrades while nanoGPT retains near-optimal performance — the non-Markovian advantage — revealing that the transformer implicitly exploits non-Markovian structure that the Markovian dual filter cannot represent. A perturbation study (Sec. C.2) further shows that the sparsity of the optimal control weights is model-dependent rather than algorithmic.

Several limitations point to directions for future work. First, the explicit optimal control formula is obtained only for the Markovian case ($\tau = 1$) in the nonlinear model. Second, the framework is entirely model-based: the parameters (A, C, μ) are assumed known, and developing a learning framework to estimate either these parameters or control weights directly from data is ongoing work.

The non-Markovian advantage identifies a precise gap: the Markovian dual filter is insufficient, and a non-Markovian nonlinear extension is needed — the linear Gaussian results of Sec. 2 and the dual filter framework provide the mathematical foundation for this next step.

References

- [1] Mary Phuong and Marcus Hutter. Formal algorithms for transformers. *arXiv preprint arXiv:2207.09238*, 2022.
- [2] Borjan Geshkovski, Cyril Letrouit, Yury Polyanskiy, and Philippe Rigollet. A mathematical perspective on transformers. *arXiv preprint arXiv:2312.10794*, 2023.
- [3] Borjan Geshkovski, Philippe Rigollet, and Domènec Ruiz-Balet. Measure-to-measure interpolation using transformers. *arXiv preprint arXiv:2411.04551*, 2024.
- [4] Álvaro Rodríguez Abella, João Pedro Silvestre, and Paulo Tabuada. The asymptotic behavior of attention in transformers. *arXiv preprint arXiv:2412.02682*, 2024.
- [5] Daniel Owusu Adu and Bahman Ghahsifard. Approximate controllability of continuity equation of transformers. *IEEE Control Systems Letters*, 2024.
- [6] Valérie Castin, Pierre Ablin, José Antonio Carrillo, and Gabriel Peyré. A unified perspective on the dynamics of deep transformers. *arXiv preprint arXiv:2501.18322*, 2025.
- [7] Kağan Akman, Naci Saldı, and Serdar Yüksel. An optimal control approach to transformer training. *arXiv preprint arXiv:2603.09571*, 2026.
- [8] Kelvin Kan, Xingjian Li, Benjamin Zhang, Tuhin Sahai, Stanley Osher, and Markos Katsoulakis. Optimal control for transformer architectures: Enhancing generalization, robustness and efficiency. In *The Thirty-ninth Annual Conference on Neural Information Processing Systems*.
- [9] Henri Cimetière, Maria Teresa Chiri, and Bahman Ghahsifard. Localmax dynamics for attention in transformers and its asymptotic behavior. *arXiv preprint arXiv:2509.15958*, 2025.
- [10] Vikram Krishnamurthy. Llms as high-dimensional nonlinear autoregressive models with attention: Training, alignment and inference. *arXiv preprint arXiv:2602.00426*, 2026.
- [11] Sang Michael Xie, Aditi Raghunathan, Percy Liang, and Tengyu Ma. An explanation of in-context learning as implicit bayesian inference. *arXiv preprint arXiv:2111.02080*, 2021.
- [12] Yu Bai, Fan Chen, Huan Wang, Caiming Xiong, and Song Mei. Transformers as statisticians: Provable in-context learning with in-context algorithm selection. *Advances in neural information processing systems*, 36:57125–57211, 2023.
- [13] Raanan Y Rohekar, Yaniv Gurwicz, and Shami Nisimov. Causal interpretation of self-attention in pre-trained transformers. *Advances in Neural Information Processing Systems*, 36:31450–31465, 2023.
- [14] Ahmed M Alaa and Mihaela van der Schaar. Attentive state-space modeling of disease progression. *Advances in neural information processing systems*, 32, 2019.
- [15] Binh Tang and David S Matteson. Probabilistic transformer for time series analysis. *Advances in neural information processing systems*, 34:23592–23608, 2021.
- [16] Gautam Goel and Peter Bartlett. Can a transformer represent a kalman filter? In *6th Annual Learning for Dynamics & Control Conference*, pages 1502–1512. PMLR, 2024.
- [17] Zhe Du, Haldun Balim, Samet Oymak, and Necmiye Ozay. Can transformers learn optimal filtering for unknown systems? *IEEE Control Systems Letters*, 7:3525–3530, 2023.
- [18] Heng-Sheng Chang and Prashant G Mehta. Dual filter: A mathematical framework for inference using transformer-like architectures. *arXiv preprint arXiv:2505.00818*, 2025.
- [19] Yaakov Bar-Shalom, X Rong Li, and Thiagalingam Kirubarajan. *Estimation with applications to tracking and navigation: theory algorithms and software*. John Wiley & Sons, 2001.
- [20] Albert Gu and Tri Dao. Mamba: Linear-time sequence modeling with selective state spaces. *arXiv preprint arXiv:2312.00752*, 2023.

- [21] Jin Won Kim, Prashant G. Mehta, and Sean Meyn. What is the Lagrangian for nonlinear filtering? In *2019 IEEE 58th Conference on Decision and Control (CDC)*, pages 1607–1614, Nice, France, 12 2019. IEEE.
- [22] Jin Won Kim and Prashant G Mehta. Duality for nonlinear filtering ii: Optimal control. *IEEE Transactions on Automatic Control*, 69(2):712–725, 2023.
- [23] Alain Bensoussan. *Estimation and control of dynamical systems*, volume 48. Springer, 2018.
- [24] Thomas Kailath, Ali H Sayed, and Babak Hassibi. *Linear estimation*. Prentice Hall, 2000.
- [25] Emanuel Todorov. General duality between optimal control and estimation. In *2008 47th IEEE conference on decision and control*, pages 4286–4292. IEEE, 2008.
- [26] Jin Won Kim and Prashant G Mehta. The arrow of time in estimation and control: Duality theory beyond the linear gaussian model. *IEEE Control Systems*, 45(2):70–90, 2025.
- [27] Andrej Karpathy. nanogpt: The simplest, fastest repository for training/finetuning medium-sized gpts. <https://github.com/karpathy/nanoGPT>, 2024.
- [28] Reginald Zhiyan Chen, Heng-Sheng Chang, and Prashant G Mehta. Differentiable filtering for learning hidden markov models. In *8th Annual Learning for Dynamics and Control Conference*, 2026.

A Explicit formulae for the dual optimal control problem in Sec. 3.1

This section provides explicit expressions for the BSΔE dual control system, the optimal control objective, and the formula for optimal control. Additional details and background on these can be found in [18]. We follow closely the notation of [18]. Denote

$$c(x) := [C(x, 1) - C(x, 0) \quad C(x, 2) - C(x, 0) \quad \dots \quad C(x, m) - C(x, 0)]^\top, \quad x \in \mathbb{S}.$$

Dual Control System. The dual control system is a backward stochastic difference equation (BSΔE) as follows:

$$Y_t(x) = (AY_{t+1})(x) + c^\top(x)(U_t + V_t(x)) - V_t^\top(x)e(Z_{t+1}), \quad x \in \mathbb{S}, \quad t = 0, 1, \dots, T-1, \quad (10a)$$

$$Y_T(x) = f(x), \quad x \in \mathbb{S}. \quad (10b)$$

Here $f : \mathbb{S} \rightarrow \mathbb{R}$ is the terminal condition and $U := \{U_t : 0 \leq t \leq T-1\} \in \mathcal{U}$ is the control input (these are both given). The BSΔE is solved to obtain the solution pair

$$Y := \{Y_t(x) : Y_t(x) \in \mathbb{Z}_t, \quad x \in \mathbb{S}, \quad 0 \leq t \leq T\},$$

$$V := \{V_t(x) : V_t(x) \in \mathbb{Z}_t, \quad x \in \mathbb{S}, \quad 0 \leq t \leq T-1\},$$

where for each fixed $x \in \mathbb{S}$, $Y_t(x)$ is real-valued and $V_t(x)$ is \mathbb{R}^m -valued. The solution pair is denoted by (Y, V) . Its existence and uniqueness is shown in [18, Prop. 8].

Optimal Control Objective. The optimal control objective is defined as follows:

$$J_T(U; f) := \text{var}(Y_0(X_0)) + \mathbb{E}\left(\sum_{t=0}^{T-1} l(Y_{t+1}, V_t, U_t; X_t)\right),$$

where $\text{var}(Y_0(X_0)) = \mathbb{E}(|Y_0(X_0) - \mu(Y_0)|^2) = \mu(Y_0^2) - \mu(Y_0)^2$ (note that Y_0 is a deterministic function), and the running cost $l : \mathbb{R}^d \times \mathbb{R}^{m \times d} \times \mathbb{R}^m \times \mathbb{S} \rightarrow \mathbb{R}$ is given by,

$$l(y, v, u; x) := (\Gamma y)(x) + (u + v(x))^\top R(x)(u + v(x)), \quad y \in \mathbb{R}^d, \quad v \in \mathbb{R}^{m \times d}, \quad u \in \mathbb{R}^m, \quad x \in \mathbb{S}.$$

where

$$(\Gamma f)(x) := \sum_{y \in \mathbb{S}} A(x, y) f^2(y) - (Af)^2(x), \quad x \in \mathbb{S},$$

$$R(x) := \text{diag}(c(x)) + C(x, 0)(I + \mathbf{1}\mathbf{1}^\top) - c(x)c^\top(x), \quad x \in \mathbb{S},$$

and $v(x)$ is the x -th column vector of the $m \times d$ matrix $v = [v(1) \quad \dots \quad v(x) \quad \dots \quad v(d)]_{m \times d}$.

Optimal control formula. The explicit expression for the function ϕ introduced in (9a) is

$$\phi(y, v; \rho) := -\rho(R)^\dagger (\rho((c - \rho(c))y) - \rho(Rv)), \quad y \in \mathbb{R}^d, v \in \mathbb{R}^{m \times d}, \rho \in \mathcal{P}(\mathbb{S}).$$

Here, $\rho(R)^\dagger$ denotes the pseudo-inverse of the $m \times m$ matrix $\rho(R) := \sum_{x \in \mathbb{S}} \rho(x)R(x)$ and the other two terms are $\rho((c - \rho(c))y) := \sum_{x \in \mathbb{S}} \rho(x)(c(x) - \rho(c))y(x)$ and $\rho(Rv) := \sum_{x \in \mathbb{S}} \rho(x)R(x)v(x)$ which are $m \times 1$ vectors.

The formula is used to compute the attention weights described in the numerical experiments.

B Proofs

B.1 Proof of the Prop. 1 (duality principle for non-Markovian linear Gaussian model)

First, using the observation process (2b), state process equation (2a) and the backward process (dual control system) (3), we compute

$$y_T^\top X_T = y_0^\top X_0 - \sum_{t=0}^{T-1} u_t^\top Z_{t+1} + \sum_{t=0}^{T-1} u_t^\top W_{t+1} + \sum_{t=1}^T y_t^\top B_t$$

Now, noting the terminal condition of the dual state $y_T = f$, and the definition of estimator S_T in (1), we get

$$f^\top X_T - S_T = y_0^\top (X_0 - \mu_0) + \sum_{t=1}^T y_t^\top B_t + \sum_{t=0}^{T-1} u_t^\top W_{t+1} \quad (11)$$

Next, we square this equation and take expectations. Since $X_0 - \mu_0 \sim \mathcal{N}(0, \Sigma_0)$, $B_t \sim \mathcal{N}(0, Q)$, $W_t \sim \mathcal{N}(0, R)$, and X_0, B, W are mutually independent, all three terms on the right hand side of (11) are zero-mean and mutually uncorrelated. Therefore,

$$\mathbb{E} \left[|f^\top X_T - S_T|^2 \right] = |y_0|_{\Sigma_0}^2 + \sum_{t=1}^T |y_t|_Q^2 + \sum_{t=0}^{T-1} |u_t|_R^2 = 2J_T(u; f)$$

and this concludes the proof. \square

B.2 Proof of Thm. 2 (solution of the linear optimal control problem)

Let $u^{(\text{opt})}$ denote the optimal control and consider an arbitrary perturbation Δu . The perturbed control trajectory can be written as $u = u^{(\text{opt})} + \Delta u$. Since the dual control system (3) is linear, the resulting dual state y will be of the form $y = y^{(\text{opt})} + \Delta y$. Here, $y^{(\text{opt})}$ and Δy are the unique solutions to the dual dynamics corresponding to $u^{(\text{opt})}$ (with terminal condition $y_T^{(\text{opt})} = f$) and Δu (with terminal condition $\Delta y_T = 0$), respectively. Now, the cost functional $J_T(u; f)$ can be expanded around $u^{(\text{opt})}$ as follows:

$$J_T(u; f) = J_T(u^{(\text{opt})}; f) + \mathcal{I}_T(u^{(\text{opt})}, \Delta u) + J_T(\Delta u; 0)$$

where $J_T(u^{(\text{opt})}; f)$ represents the minimum cost, $J_T(\Delta u; 0)$ is the second-order error term (always non-negative due to convexity), and the first-order variation (cross terms) is given by:

$$\mathcal{I}_T(u^{(\text{opt})}, \Delta u) = (y_0^{(\text{opt})})^\top \Sigma_0 (\Delta y_0) + \sum_{t=1}^T (y_t^{(\text{opt})})^\top Q (\Delta y_t) + \sum_{t=0}^{T-1} (u_t^{(\text{opt})})^\top R (\Delta u_t)$$

Using the definition of the forward momentum process η from (6b) and the dual control system dynamics for Δy , we can simplify the first-order variation into the following inner product form:

$$\mathcal{I}_T(u^{(\text{opt})}, \Delta u) = \sum_{t=0}^{T-1} \left(C\eta_t + Ru_t^{(\text{opt})} \right)^\top (\Delta u_t)$$

The optimality of $u^{(\text{opt})}$ requires that the first-order variation $\mathcal{I}_T(u^{(\text{opt})}, \Delta u)$ must vanish for any arbitrary perturbation Δu . This implies $u_t^{(\text{opt})} = -R^{-1}C\eta_t$ for all $t \in \{0, \dots, T-1\}$, which gives us the optimal control formula (6c). Also, the strict convexity of the cost functional with respect to u ensures that this stationary point is the unique global minimizer. This completes the proof. \square

B.3 Proof of Prop. 4 (well-posedness of the nonlinear predictor representation)

The existence theorem relies on the following proposition from linear algebra.

Proposition 9 (See [18, Prop. 28]). *Let $s : \mathbb{O} \rightarrow \mathbb{R}$. Then there exists unique $(\bar{s}, \tilde{s}) \in \mathbb{R} \times \mathbb{R}^m$ such that the following decomposition holds:*

$$s(z) = \bar{s} + \tilde{s}^\top e(z), \quad z \in \mathbb{O}.$$

Explicitly,

$$\bar{s} := \frac{1}{m+1} \sum_{z \in \mathbb{O}} s(z), \quad \text{and} \quad \tilde{s}(i) = (s(i) - \bar{s}), \quad i = 1, 2, \dots, m.$$

Example 10 ($m=1$). *Let $s : \{0, 1\} \rightarrow \mathbb{R}$. Denote $s^+ := s(1)$ and $s^- := s(0)$. Then*

$$s(z) = \bar{s} + \tilde{s} e(z), \quad z \in \{0, 1\},$$

where $\bar{s} := 0.5(s^+ + s^-)$ and $\tilde{s} := 0.5(s^+ - s^-)$ (recall $e(1) = 1$ and $e(0) = -1$).

We now provide a proof of Prop. 4, establishing well-posedness of the nonlinear predictor representation in Prop. 4. The proof follows the analogous result for the HMM in [18].

Proof of Prop. 4. Let S_T be any \mathcal{Z}_T -measurable random variable. From Doob-Dynkin lemma, there exists a deterministic function $s : \mathbb{O}^T \rightarrow \mathbb{R}$ such that

$$S_T = s(Z_1, \dots, Z_{T-1}, Z_T).$$

Set $S(z) := s(Z_1, \dots, Z_{T-1}, z)$, for $z \in \mathbb{O}$. Using Prop. 9,

$$S_T = S(Z_T) = S_{T-1} - (U_{T-1})^\top e(Z_T),$$

where

$$S_{T-1} = \frac{1}{m+1} \sum_{z \in \mathbb{O}} S(z), \quad U_{T-1}(i) := -(S(i) - S_{T-1}), \quad i = 1, 2, \dots, m.$$

Uniqueness is from the uniqueness of the decomposition. The proof is completed through induction by repeating the procedure for $S_{T-1} \in \mathcal{Z}_{T-1}$.

Now, the conditional expectation is meaningfully defined only for sample paths $Z = z$ with $\mathbb{P}([Z = z]) > 0$. Note here that because $|\mathbb{O}| = m+1$ and T are both finite, there are only finitely many—specifically $(m+1)^T$ —sample paths. Thus, $\mathbb{P}([Z = z])$ is a well-defined object for each sample path, although it may be zero depending on the model properties.

There are two ways to address this issue:

1. Assume $\mathbb{P}([Z = z]) \geq \underline{c}^T > 0$ for all $z \in \mathbb{O}^T$, and the existence of a unique U follows directly from the earlier result.
2. Adopt the convention $\frac{0}{0} = 0$ to define (or extend) the conditional expectation for sample paths $Z = z$ with $\mathbb{P}([Z = z]) = 0$. Then again, a particular selection of U follows from the above result.

In the second case, however, there may be other choices of U such that the representation (4) holds: Any two choices will yield a representation that coincides on the set $\{z \in \mathbb{O}^T : \mathbb{P}(Z = z) > 0\}$ but may differ on the set $\{z \in \mathbb{O}^T : \mathbb{P}(Z = z) = 0\}$. ■

Example 11 ($m=1$). *Set $S_T^+ = s(Z_1, \dots, Z_{T-1}, 1)$ and $S_T^- = s(Z_1, \dots, Z_{T-1}, 0)$. Then $S_T^+, S_T^- \in \mathcal{Z}_{T-1}$ and*

$$S_T = S_{T-1} - U_{T-1} e(Z_T),$$

where $S_{T-1} = 0.5(S_T^+ + S_T^-)$ and $U_{T-1} = -0.5(S_T^+ - S_T^-)$.

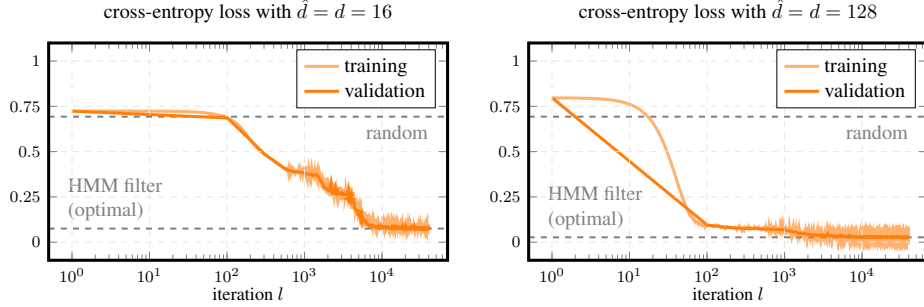


Figure 5: Training and validation loss curves for the transformer model. The loss converges to the optimal filter loss in both settings of $d = \hat{d} = 16$ (left) and $d = \hat{d} = 128$ (right). The colored solid lines represent the training (light) and validation (dark) loss curves, while the dashed lines indicate the optimal filter loss (dashed line) and the loss of uniformly random guessing (dashed line).

C Numerical Experiments

C.1 Training Details for nanoGPT

We train nanoGPT [27], a lightweight GPT implementation, on synthetic datasets generated from HMMs. Training is performed using the AdamW optimizer with learning rate 10^{-3} and parameters $\beta_1 = 0.9$ and $\beta_2 = 0.99$ for 40,000 iterations. To accelerate convergence, the first 4,000 iterations are used for learning-rate warmup, after which the learning rate remains constant. The dropout rate is set to 10^{-2} . Representative loss curves for $d = 16$ and $d = 128$ are shown in Figure 5, demonstrating that nanoGPT converges to the optimal filtering loss in both settings (the embedding dimension $\hat{d} = d$ in both cases). These training hyperparameters are used for all nanoGPT experiments in this work.

C.2 Model perturbation study

In this experiment, we investigate the robustness of the dual filter control weights and nanoGPT attention weights under model perturbations. The model parameters are perturbed via a convex combination of the nominal parameters and a uniform distribution, where the perturbation level $\varepsilon \in [0, 1]$ determines the deviation from the nominal model. We consider perturbations to either the transition matrix or the emission matrix (but not both together). The transition matrix perturbation are as follows

$$A(x, x') = (1 - \varepsilon)A_{\text{nominal}}(x, x') + \frac{\varepsilon}{d}, \quad x, x' \in \mathbb{S}, \quad (12a)$$

and the emission matrix is perturbed as follows

$$C(x, z) = (1 - \varepsilon)C_{\text{nominal}}(x, z) + \frac{\varepsilon}{m + 1}, \quad x \in \mathbb{S}, \quad z \in \mathbb{O}. \quad (12b)$$

The nominal model is illustrated in Fig. 2. In (12a) and (12b), the second terms correspond to uniform distributions added to the respective model parameters. As ε increases, the model deviates further from the nominal, smoothing the deterministic cycle structure, allowing us to assess how the control and attention patterns change. Fig. 6 depicts the control and attention patterns under three representative perturbation levels: $\varepsilon = 0.01$, $\varepsilon = 0.1$, and $\varepsilon = 0.2$. The nanoGPT is trained separately for each perturbation level to ensure that the attention patterns are learned under the corresponding data generated from the perturbed model conditions.

The results of this study indicate that the structure of the optimal control weights are sensitive to model perturbations. Even small perturbations to the state transition parameter A cause the dual filter’s control weights to shift from a vertical, event-driven pattern to a sparse but diagonal one. This diagonal structure indicates that the filter is aggregating evidence across multiple past cycles rather than relying solely on a single branching moment. In contrast, the attention weights of nanoGPT remain sparse and vertical across these perturbations. Despite this structural difference, the transformer demonstrates inherent robustness by maintaining near-optimal loss that closely matches the dual filter. On the other hand, perturbations to the emission parameter C have less impact on the weights, which remain focused on the informative time steps where $Z_t = 1$ across all perturbation levels, albeit with increasing diffuseness as ε grows.

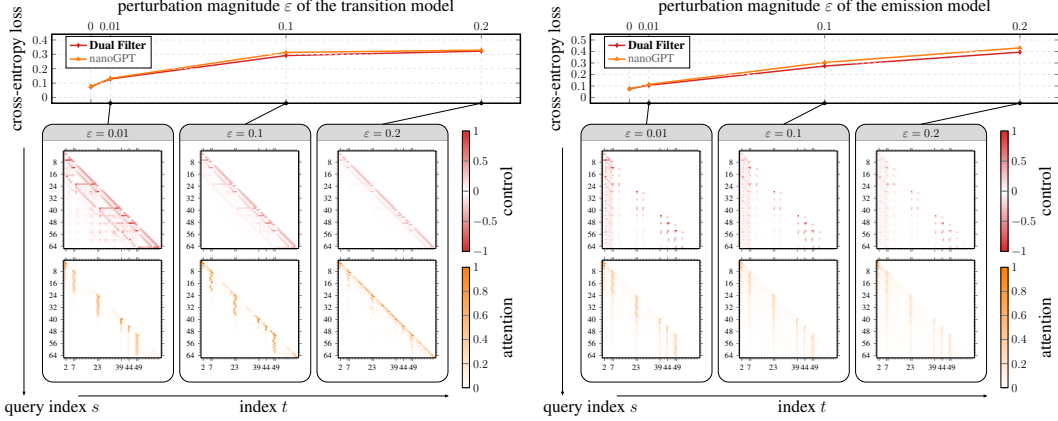


Figure 6: Control and attention patterns shift under model perturbation. The model parameters are perturbed via a convex combination of the nominal parameters and a uniform distributed probability matrix, with a perturbation level of $\varepsilon \in [0, 1]$ following (12). The perturbation from left to right is $\varepsilon = 0.01$, $\varepsilon = 0.1$, and $\varepsilon = 0.2$, and the perturbation of the transition matrix is shown on the left while the perturbation of the emission matrix is shown on the right. The cross-entropy loss of the learned nanoGPT remains near-optimal across all perturbation levels, closely matching the dual filter’s loss, indicating that the transformer maintains robust performance even as the data generated from the perturbed model. The top rows show the dual filter control weights computed with the perturbed model parameters, while the bottom rows show the attention matrix from a trained transformer under the same model perturbation. The major ticks in the index axis of the heatmaps correspond to the time steps where $Z_t = 1$; the minor ticks correspond to the time steps where $Z_t = 0$.

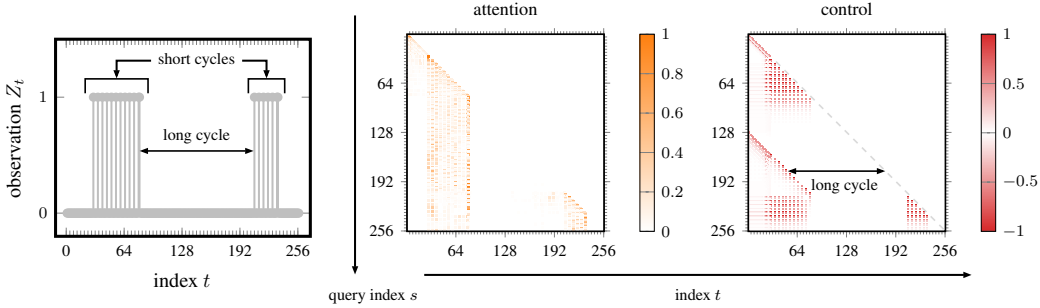


Figure 7: A sample observation trajectory and the corresponding control and attention patterns for the higher-dimensional system. The figure on the left shows a sample observation trajectory, where it shows both the shorter cycle and the longer cycle. The middle figure shows the attention weights from the trained nanoGPT, and the right figure shows the control weights from the dual filter. Both the attention and control weights exhibit a sparse pattern that is non-zero at the time indices when 1s are observed in the data. Additionally, the control weights also show a periodic pattern that reflects the underlying longer cycle structure of the data. The gray dashed line indicates the diagonal in the control heatmap.

C.3 A higher-dimensional system

The two-cycle HMM from Sec. 4 is used with $d = 128$, $T = 256$, and $q = 4$. A nanoGPT is trained on this HMM data, consistent with the training details in Sec. C.1. Fig. 7 depicts a sample observation trajectory, and the corresponding control and attention weights. Similar to the lower-dimensional case in the main text, the controls and attentions exhibit a sparse pattern that is non-zero at the time indices when 1s are observed in the data. An interesting observation is that the controls in this case also show a periodic pattern that is not observed in the lower-dimensional case.